

HIGH ALTITUDE LIDAR TO ENHANCE GEOSAR SYSTEM PERFORMANCE

R.B. Haarbrink

EarthData Technologies, 9625 Surveyor Court, Suite 330, Manassas, VA 20110, U.S.A.
rhaarbrink@earthdata.com

KEY WORDS: LIDAR, GeoSAR, Data Fusion, Calibration and Validation, Derivations of Forest and Vegetation Parameters, Digital Surface Models, Filtering

ABSTRACT:

EarthData Technologies has performed a research and development project to investigate the possibilities of a co-mounted LIDAR system to enhance the performance of the Geographic Synthetic Aperture Radar (GeoSAR) system. The LIDAR system could provide precise ground control points that can be used in the mosaick process and it could add valuable information about tree canopy structures to the process of merging the X-band and P-band data, which would improve the Digital Elevation Model (DEM) accuracy of the GeoSAR system. Therefore, an off-the-shelf ALS40 unit manufactured by Leica Geosystems was tested in profiling mode at 10 km above terrain. The LIDAR profiler was capable of consistently producing range measurements from that altitude with a vertical precision of 26 cm (1 sigma), after applying a special bore sight method that had been developed by EarthData Technologies. Although the high altitude LIDAR system was not able to penetrate through clouds, it did penetrate through vegetation to map the underlying ground level at the same rate as a LIDAR system operating from lower altitudes. Finally, a method was developed to approximate the “thickness” of the vegetation by waveform simulation from a multiple return system. The results of the high altitude LIDAR tests are presented in this paper.

1. INTRODUCTION

GeoSAR is a dual-frequency, dual-polarimetric, interferometric airborne radar mapping system that generates DEMs and orthorectified radar reflectance maps near the tops of trees as well as beneath foliage. The GeoSAR system is mounted on a Gulfstream-II jet aircraft and collects radar data in two frequencies. The X-band maps the first surface, near the top of trees and the P-band maps beneath the foliage and assists in the production of a bare-earth terrain model and the detection of structures beneath trees.

The system has been designed to record simultaneous X-band and P-band data in two 10 km wide swaths on the left and right sides of the aircraft when flying at 10 km above ground level. The X-band antennas are mounted under the wings close to the fuselage, while the P-band antennas are mounted on the wingtips. In this configuration, each X-band and P-band antenna provides two looks at each point on the ground for a total of four looks on each side (Figure 1). GPS and IMU units are used for the aircraft navigation solution and to measure the position and motion of the wingtip antennas.

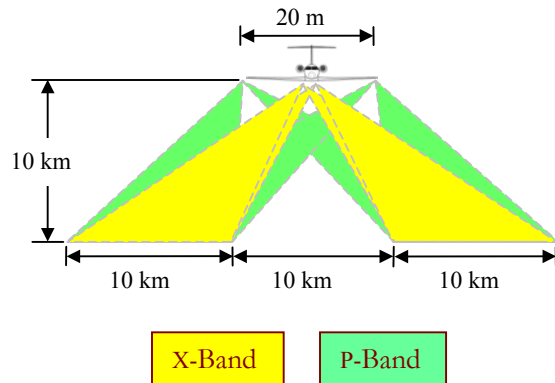


Figure 1. GeoSAR system configuration

The left-right look angles on each side of the aircraft combined with the mosaicking process mitigates radar shadow and layover. The GeoSAR system has been designed for day/night, all-weather, rapid and large-area data collection. As it is a single-pass system, it compensates for challenges of repeat-pass processing, which include temporal decorrelation, atmospheric distortion, and motion compensation and calibration issues. More information on the capabilities and limitations of IFSAR in general and GeoSAR in particular can be found in Maune (2001).

GeoSAR DEMs and images support many different products and can be viewed using standard software, such as IMAGINE, ArcInfo, ArcView, ImageStation, ATLAS and DAT/EM (Hoffman et al, 2003). Some products that can be derived from GeoSAR DEMs and images include DEMs for orthophoto rectification, planimetric maps with 3-meter resolution, topographic maps with 3-meter contour intervals and land-use/land-cover mapping to show roads, structures and variations in crop types and other vegetation. For example, Figure 2 shows a 3-meter X-band reflectance map of a wetland area in California and a fully compliant 1:50,000 topographic line map of the same area extracted stereoscopically using the reflectance map and its orthomate on an ImageStation SSK (top and bottom, respectively).

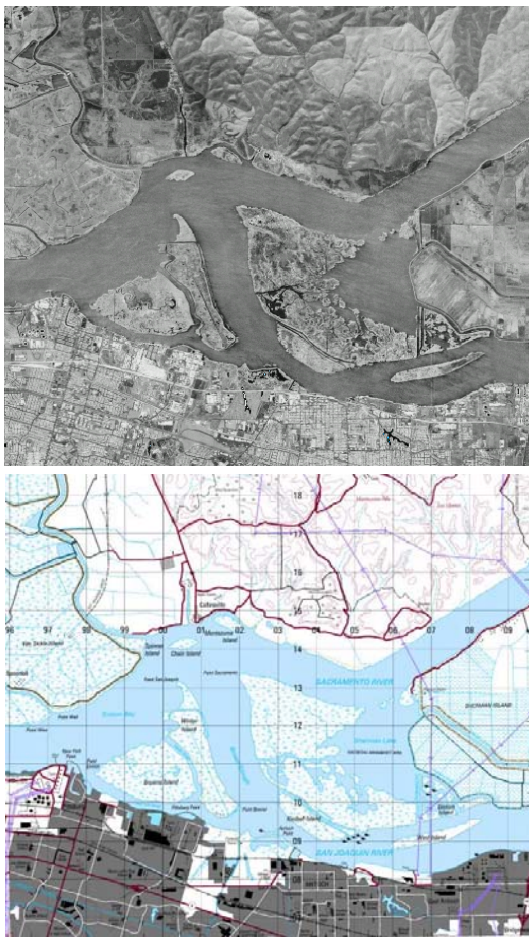


Figure 2. 3-Meter X-band reflectance map (top) and topographic map (bottom)

The DEM vertical precision from the X-band varies between 0.5 and 1.2 meter and from the P-band between 1 and 4 meter (both 1 sigma), depending on the type of terrain and the density of the foliage. Airborne laser-scanning systems, or LIDAR systems, are also capable of measuring the canopy top and the underlying ground surface, however, the DEM vertical

precision from LIDAR is generally better than 0.15 meter (e.g. Huising and Gomes Pereira, 1998; Schenk et al, 2001; Crombaghs et al, 2002). The LIDAR data acquisition rate, on the other hand, is limited compared to the rapid GeoSAR data collection at 100 km² per minute, which is at least ten times faster than normal LIDAR data collection and therefore makes the GeoSAR system much more efficient for large areas and forests.

Comparison studies between LIDAR and X-band data from other radar mapping systems show that LIDAR provides a more precise definition of the terrain, particularly in urban cores (Canfield and Samaranayake, 1996; Kleusberg and Klaedtke, 1999; Mercer and Schnick, 1999; Sties et al, 2000; Wang et al, 2001). Where the comparison studies between LIDAR and X-band radar systems were all based on datasets collected on separate missions with independent platforms, EarthData Technologies has performed a research and development project to investigate the possibilities of a co-mounted LIDAR system to enhance GeoSAR system performance. The LIDAR system can provide precise ground control points that can be used in the mosaick process, and it can add valuable information about tree canopy structures to the process of merging the X-band and P-band data, which would improve the DEM accuracy of the GeoSAR system. An off-the-shelf ALS40 unit manufactured by Leica Geosystems of Westford, Massachusetts was tested in profiling mode at 10 km above terrain. The results of the high altitude LIDAR tests are presented in this paper.

2. HIGH ALTITUDE LIDAR TESTS

The high altitude LIDAR test flights had the following objectives:

- To determine if the system provides sufficient power to allow operations from 10 kilometers above terrain, and if so,
- To develop a bore sight method for a high altitude profiling LIDAR,
- To determine the system's accuracy, return percentages and SNR,
- To investigate the limits of a high altitude profiling LIDAR under variable visibility and cloud situations, and
- To analyze the signal penetration performance with variable vegetation types.

2.1 LIDAR Test System And Aircraft

The prototype ALS40 has been designed to perform up to a maximum of 6 km above terrain, so for this particular test certain electronics, such as the range boards, were adjusted for operations up to 10 km. The system has a standard 4-Watt laser transmitting pulses with a peak power of 0.15 mJ and a width of 8.5 ns, and records up to three returns with intensity per outgoing pulse. Although the ALS40 is capable of

recording 50,000 pulses per second at lower altitudes, the pulse rate had to be decreased to 8 kHz, because the usable maximum laser pulse rate is limited to the point where the roundtrip time plus the processor and timing overhead equal the inter-pulse period. Nevertheless, the 8 kHz pulse rate still results in a very small post spacing of about 2 cm in profiling mode with a 3-meter footprint diameter from 10 km above the terrain. The estimated Signal-to-Noise-Ratio (SNR) was 5.3 for a 10% diffuse target under clear skies and the vertical precision, including error budgets from GPS, IMU, encoder and range uncertainties, was estimated to be 34 cm.

The aircraft for the high altitude test flights was a Cessna 441 Conquest II Propjet with a pressurized cabin (Figure 3), which caused no interconnection with the existing GeoSAR system and did not adversely affect GeoSAR operation capability. The aircraft was equipped with a CCNS flight navigation management system and had been, especially for this test, outfitted with a special coated anti-reflection (AR) window to minimize absorption of the 1064 nm infrared laser light. All test flights were conducted with a GPS base station positioned on an NGS Primary Airport Control point for precise DGPS positions.



Figure 3. Cessna 441 Conquest II propjet in preparation for high altitude LIDAR test flights

2.2 First Test Flights

The first flight lines were acquired in swath mode starting from 5 km above terrain at increments of 1 km up to 10 km above terrain. First returns were recorded for 93% of pulses transmitted from a flying height of 10 km, while the remaining 7% of outgoing pulses that did not produce any returns are thought to have been in areas of open water. Second returns were recorded for 15% of outgoing pulses. In addition to the six overlapping flight lines, the aircraft was gradually rolled from 0 to 15° at an altitude of 10 km with the Field-Of-View (FOV) set to 65°, which induced slant ranges as long as about 15 km. At first glance it appeared that drop-outs were beginning to occur at the very longest ranges. It was concluded that the first

objective of the test - to determine if a LIDAR system can provide data from 10 km above terrain - had been successfully met.

3. BORE SIGHTING APPROACH

Consecutive test flights were performed to address the remaining four objectives. First, the high altitude profiler had to be calibrated, or bore sighted, which is necessary to align the IMU and the LIDAR coordinate reference frames. EarthData Technologies has designed a special bore sight method for a profiling LIDAR, because the standard procedures used for swath data are not applicable. The bore sight plan for a profiling LIDAR consists of two flight lines collected over a large topographic feature with an open and evenly sloped surface. One flight line is flown perpendicular to the hillside (for pitch correction), while the second flight line is flown along the hillside (for roll correction). Both flight lines are flown twice in opposite directions.

Figure 4 shows the four profiles from 10 km over the face of a large topographic feature (Stone Mountain in North Carolina) that is about 500 meters high and wide. The profiles have hit the target area extremely well. The underlying hillshade was derived from LIDAR data collected at a much lower flying height in swath mode.

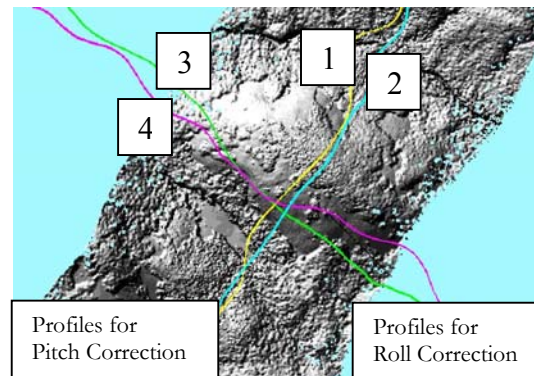


Figure 4. Profiles over a large topographic feature

Pitch was corrected using the two bi-directional profiles that run to the northeast and to the southwest over the top of the mountain (yellow line 1 and blue line 2). Figure 5 illustrates the pitch correction. The same yellow and blue profiles 1 and 2 are the unadjusted two bi-directional cross-slope profiles before the actual pitch correction was applied. Both profiles were then iteratively brought together by adjusting the pitch angle until they overlaid each other as they should. This is illustrated by the two white arrows: the blue profile shifts to the right and the yellow profile moves by the same distance towards the blue profile. The green and purple points are from the two perpendicular profiles 3 and 4 (which were not used for the pitch correction).

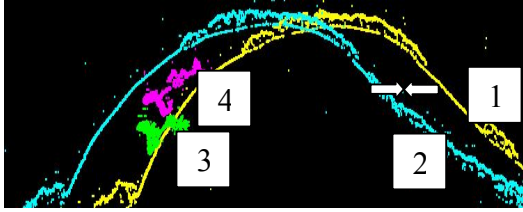


Figure 5. Pitch correction

The roll offset was measured and iterated to full alignment using the two bi-directional profiles that run to the northwest and to the southeast along the sloped surface (green line 3 and purple line 4). The roll correction is depicted in Figure 6, showing the alignment of the profiles before and after the roll correction.

Having determined the bore sight parameters, the validity of the correction angles was tested by applying the bore sight parameters to two flight lines in swath mode. The two flight lines were bi-directionally collected over an airport from only 1500 meters above terrain with a 45° FOV. The apparent pitch and roll errors were corrected with a maximum relative vertical error of less than 15 cm in open and flat areas, which proved that the second objective of the test - to develop a bore sight method for a high altitude profiling LIDAR - had been successfully met.

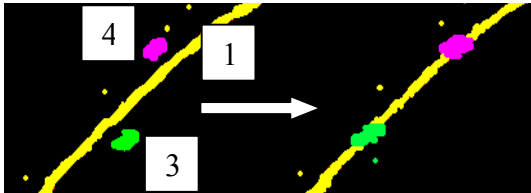


Figure 6. Roll correction

The process flow was based on reuse of existing LIDAR production processes. The position and orientation calculations were done with PosProc from Applanix; the raw LIDAR point generation and the bore sight corrections were done with the ALS40 Post Processor; and the actual bore sight measurements were performed using TerraScan and TerraModeler software in conjunction with Microstation.

4. DATA ANALYSIS

4.1 Vertical Accuracy

The vertical accuracy of the high altitude profiles was determined by comparison of the LIDAR data against a network of ground control points on the open, flat and homogeneous sites in the vicinity of the runway. The six hundred ground control points were surveyed

at the airport, using one GPS base station and two roving GPS receivers with event timing capability.

The vertical precision of the high altitude profiler does not seem to degrade with increasing altitude and is repeatedly better than 26 cm (1 sigma). This result exceeds the estimated height error at nadir of 34 cm, which is probably caused by smoothing of the surface roughness by the large footprint. The RMSE values are identical to the standard deviations indicating removal of vertical bias. The planimetric precision had not been verified, but based on statistical models, the 1-sigma error in X and Y is estimated to be better than 74 cm.

4.2 Return Percentages

In addition to the accuracy assessment, the exact percentages of returns per transmitted laser pulse have been analyzed. Up to 99% of outgoing pulses generated first returns, 36% produced second returns and 1% measured third returns. Although the return percentages vary with the terrain type and the length of the flight lines, the high altitude profiler has at least as many first and second returns as a regular LIDAR system, which indicates that the return performance of a high altitude profiler has not degraded. However, thicker vegetation will make it harder to penetrate to the ground from higher altitudes and therefore will reduce the number of second and third returns. The return percentages degraded to zero when flying over total (thin) cloud cover. The system was able to record the top of a few scattered clouds without signal penetration, but as expected, the 1064 nm laser light is not able to penetrate clouds.

4.3 Signal to Noise Ratio

The intensity information of each return can be used as an additional discriminator of objects on the ground and assist in classification, filtering and strip adjustment operations (Maas, 2001). For this project however, the intensity readings were used to approximate the actual SNR of the high altitude profiler. As for digitizing the actual SNR, the closest approximation would be given by:

$$SNR = \frac{I_{avg} \cdot V_{max}}{I_{max} \cdot \sigma_N} \quad (1)$$

where I_{avg} = average intensity reading
 V_{max} = maximum signal value in Volts
 I_{max} = maximum intensity value
 σ_N = typical noise level (1 sigma) in Volts

The estimated SNR values from first return intensities of the 10 km profiles over the airport and the bore sight area varied between 5.7 and 10.7. This variation may be caused by differences in terrain type and air

humidity under the canopy, and by a reduction of the first return intensity whenever a second return is present, because the available photons are being divided between the two surfaces. In a perfect world, the sum of the first return and second return intensities would be equal to the intensity of a single return from a material of the same reflectivity. However, with these two small returns, the LIDAR profiler is approaching the threshold of detection and would therefore tend to see more variation in the intensity values.

5. VEGETATION CHARACTERIZATION AND WAVEFORM SIMULATION

To analyze the signal penetration performance with variable vegetation types, high altitude profiles were flown over a vegetated area and were then compared to a comprehensive set of in situ data from field measurements. Where the high altitude profiler measured a Signal Penetration Ratio (SPR) of 0.86 over denser loblolly and longleaf pines, it recorded less penetration through the less dense pond pines, mixed pines and hardwood canopies (0.65 SPR). The SPR is the number of returns on the ground, whether first, second or third return, divided by the total number of transmitted pulses. More dense vegetation would normally imply a lower SPR, however the pond and mixed pines sections have more second and third returns from underlying lower vegetation rather than from the underlying ground level.

The spatial distribution of the first and second returns from the loblolly pine section is presented in Figure 7. The first returns are represented by the yellow points and the second returns by the green points. To indicate the canopy height, one point was measured to be 6.24 m above ground level. Data analysis has also shown that a gap of 0.5 m in the canopy top allows recording of a second return through the canopy on the ground. If the gap becomes less than 0.5 m, the relative return power strength will be too weak to record a second return and penetrate the upper canopy. This is from 10 km with an illuminated footprint diameter of 3 m.

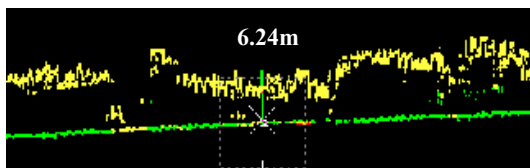


Figure 7. Spatial distribution of first and second returns from loblolly pine

In general, 50% of all returns are first returns reflected off the canopy top. Most of the ground level points were second returns, varying from 26% for pond pines to 43% for loblolly pines. Only a few third returns

were recorded on ground level (3%) for the less dense pond and mixed pines. All these numbers confirm that a high altitude profiler to enhance GeoSAR system performance requires at least a multiple return system recording up to three returns. If the profiler were to measure the “thickness” of different canopy levels, the waveform digitizing approach would be potentially more beneficial.

In this study, a waveform simulation of the returning pulse from five different vegetation types was developed by slicing the return heights into incremental height ranges of 10 cm, counting the number of returns in each height range and consequently generating a “thickness” plot of the particular vegetation type. By counting a large number of returns from the same vegetation type, the resulting pattern should approximate the average waveform from one returned pulse in the same area, while the number of returns in each height range should approximate the amplitudes of the waveform. Figure 8 presents the simulated waveform of the loblolly pine and its corresponding photograph. The simulated waveforms of the four other vegetation types clearly showed the characteristic differences in tree crowns and tree heights. As the resulting return signal captured in a waveform is a convolved measure of, among others, the roughness and slope of the surface, the data for the waveform simulations were chosen at flat ground level areas.

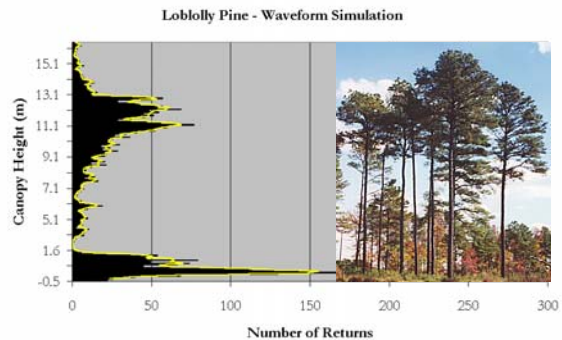


Figure 8. Simulated waveform of loblolly pine from high altitude LIDAR data

The yellow trend line was added to visualize the simulated waveform. The graph shows one major peak at ground level and three peaks between 11 and 13 meters, indicating the tree tops in this sample dataset. A waveform sample interval of 10 cm would imply a return signal digitization rate of once every 0.334 ns, which in turn would result in a maximum vegetation “depth” of 25.6 meters when one would record 256 additional bytes per signal. This obviously has major impacts on data handling and storage, depending on the update frequency chosen, and would entail a complete redesign of the system controller of the current components of the ALS40 and all other commercially available LIDAR systems, including a

new microprocessor in addition to the waveform digitizer design. In addition, it should be noted that ground returns could be missed when for example unexpected tall trees are taller than the height range recorded by the digitizer.

6. CONCLUSIONS

A series of test flights was conducted for the functional design of a profiling LIDAR that can be mounted on and operated from the GeoSAR aircraft to enhance GeoSAR system performance by providing precise ground control and valuable information about tree canopy structures. From the test series, flown from 10 km using an existing, commercially available LIDAR system from Leica Geosystems, it can be concluded that:

- The LIDAR profiler was capable of consistently producing range measurements from 10 km above terrain, and a representative number of first, second and third returns have been measured at that altitude.
- A high altitude profiling LIDAR operating at 10 km can be calibrated. However, a large topographic feature with an open and evenly sloped surface is required.
- The height accuracy assessment of the high altitude profiling LIDAR indicates that the precision is 26 cm (1 sigma) with a SNR between 5.7 and 10.4, depending on the reflectivity of the target and the existence of second returns. A ground control survey is necessary to remove the vertical bias.
- A high altitude profiling LIDAR with a wavelength of 1064 nm is not able to penetrate through clouds. When it does measure the top of scattered clouds, it does not record any returns at all when flying over a full cloud deck.
- A high altitude profiling LIDAR with the capability of recording three returns per transmitted pulse can penetrate through vegetation to map the underlying ground level. Bare earth points were recorded for 86% of outgoing pulses under loblolly and longleaf pines and for 65% under mixed pines and hardwood canopies. The "thickness" of the vegetation can be approximated by waveform simulation from a multiple return system.

REFERENCES

Canfield, D. and V.A. Samaranyake, 1996. Digital Elevation Model Test for LIDAR and IFSARE Sensors. Open File Report 96-401 of the U.S. Department of the Interior, U.S. Geological Survey, National Mapping Division.

Crombaghs, M.J.E., S.J. Oude Elberink, R. Brügemann and E.J. de Min, 2002. Assessing Height Precision of Laser Altimetry DEMs. Presented at ISPRS WG III/3 Symposium "Photogrammetric Computer Vision" in Graz.

Hoffman, G.R., R. Burrell and R. Malhotra, 2003. GeoSAR DEM Edit and Product Generation System. Presented at ASPRS Conference in Anchorage, AK.

Huising, E.J. and L.M. Gomes Pereira, 1998. Errors and Accuracy Estimates of Laser Data Acquired by Various Laser Scanning Systems for Topographic Applications. *ISPRS Journal of Photogrammetry & Remote Sensing*, 53, pages 245-261.

Kleusberg, A. and H.-G. Klaedtke, 1999. Accuracy Assessment of a Digital Height Model Derived From Airborne Synthetic Aperture Radar Measurements. In Proceedings Photogrammetric Week 1999, Wichmann, Heidelberg.

Maas, H.-G., 2001. On the Use of Pulse Reflectance Data for Laserscanner Strip Adjustment. *International Archives of Photogrammetry and Remote Sensing*, Volume XXXIV, Part 3/W4, pages 53-56. Presented at ISPRS III/3 and III/6 Workshop "Land Surface Mapping and Characterization Using Laser Altimetry" in Annapolis, MD.

Maune, D., 2001. *Digital Elevation Model Technologies and Applications: The DEM Users Manual*. Chapter 6. ASPRS, Bethesda, MD.

Mercer, J.B. and S. Schnick, 1999. Comparison of DEMs From STAR-3i Interferometric SAR and Scanning Laser. *International Archives of Photogrammetry and Remote Sensing*. Presented at ISPRS III/5 and III/2 Workshop in La Jolla, CA.

Schenk, T., S. Seo and B. Csatho, 2001. Accuracy Study of Airborne Laser Scanning Data With Photogrammetry. *International Archives of Photogrammetry and Remote Sensing*, Volume XXXIV, Part 3/W4, pages 113-118. Presented at ISPRS III/3 and III/6 Workshop "Land Surface Mapping and Characterization Using Laser Altimetry" in Annapolis, MD.

Sties, M., S. Krüger, J.B. Mercer and S. Schnick, 2000. Comparison of Digital Elevation Data From Airborne Laser and Interferometric SAR Systems. *International Archives of Photogrammetry and Remote Sensing*, Volume XXXIII, pages 866-873. Presented at ISPRS Conference in Amsterdam.

Wang, Y., B. Mercer, V.C. Tao, J. Sharma and S. Crawford, 2001. Automatic Generation of Bald Earth Digital Elevation Models from Digital Surface Models Created Using Airborne IFSAR.